Feature Article

Evaluation of different methods for the determination of the plateau modulus and the entanglement molecular weight

Chenyang Liu [a,b], Jiasong He [b], Evelyne van Ruymbeke [a,1],
Roland Keunings [c,**], Christian Bailly [a,*]

[a] *Unité de Chimie et de Physique des Hauts Polymères, Université catholique de Louvain, B-1348 Louvain-La-Neuve, Belgium*
[b] *Key Laboratory of Engineering Plastics, Joint Laboratory of Polymer Science and Materials, Institute of Chemistry,
Chinese Academy of Sciences, Beijing 100080, China*
[c] *CESAME, Université catholique de Louvain, B-1348 Louvain-La-Neuve, Belgium*

Abstract

We critically evaluate and compare all major published methods for the experimental determination of the plateau modulus for monodisperse as well as polydisperse polymers with linear architecture. For long-chain monodisperse model systems ($M_w/M_n < 1.1$ and number of entanglements > 20–30), the various methods show excellent agreement, within an error margin of 5–10% close to the experimental uncertainty. For low numbers of entanglements, the terminal peak integration method requires a careful extrapolation at the high frequency side. This is best achieved by a simple subtraction of the Rouse relaxation. The universal terminal relaxation concept is validated for long chains, in logical agreement with tube model concepts. We further analyze the extension to polydisperse polymers of the methods validated for monodisperse systems. Agreement between the methods within a 15% range can be achieved in favorable cases. The preferred method is the terminal peak integration, with the same caveats as for monodisperse samples. Predictions from tube models can nicely complement other approaches but should be used with caution because they are sensitive to errors on the experimentally determined molecular weight and distribution. Methods based on the 'crossover' modulus are only semi-quantitative. A cross-check of all available methods is the best way to achieve maximal accuracy for polydisperse systems.
© 2006 Elsevier Ltd. Open access under CC BY-NC-ND license.

Keywords: Plateau modulus; Viscoelastic properties; Tube models

1. Introduction

Since, the seminal work of de Gennes [1] and Doi and Edwards [2], tube theories have made spectacular progress and have, in a sense, become the 'standard model' of polymer physics. Because they cleverly simplify the hugely complex topological interactions between real macromolecules into a mesoscale mean field description, tube models show a unique balance of 'economy', sound physical basis and relative tractability. Their success is demonstrated by the quality of predictions made for the linear as well as non-linear

viscoelastic properties from knowledge of molecular weight distribution and architecture [3–7]. Tube models have also enabled the development of increasingly robust schemes for solving the so-called inverse problem for linear polymers, i.e. inferring the molecular distribution from the rheological response [8–16]. In all tube models, the fundamental parameter describing the topological network is the molecular weight between entanglements M_e. Hence, tube models should only require two adjustable scaling parameters, one for the time scale and one for the stress scale, both linked to M_e. The basic time scaling parameter is usually taken as τ_e, the equilibration time of a segment between entanglements. The basic stress scaling parameter is the plateau modulus G_N^0. The tube picture provides an unambiguous relationship between M_e and G_N^0, provided that consistent definitions are used. This has recently been clarified in a definitive review by Larson et al. [4]. Unfortunately, while model inconsistencies can lead to typical errors of 20% for G_N^0, experimental values (noted $G_N^0\,_{exp}$ in the remainder of the manuscript) sometimes show a much larger

---

* Corresponding authors. Tel.: +32 10 478412; fax: +32 10 451593.
E-mail addresses: roland.keunings@inma.ucl.ac.be (R. Keunings), christian.bailly@uclouvain.be (C. Bailly).
[1] Present address: Foundation for Research and Technology-Hellas (FORTH) P.O. Box 1527, 71110 Heraklion, Crete, Greece.

spread. For example, $G_{N\,\text{exp}}^0$ values ranging from 1.1 up to 2.6 MPa have been reported for polyethylene (PE) [17–26], and for bisphenol-A polycarbonate (PC), figures range from 1.2 up to 4.1 MPa [21,27–31]. The latter example is particularly revealing because no differences in molecular microstructure can be invoked to explain the situation. Clearly, the experimental evaluation of $G_{N\,\text{exp}}^0$ is in many cases the limiting factor for an accurate description of the entanglement network rather than subtle differences between models. Various methods for $G_{N\,\text{exp}}^0$ determination have been published over the years [17] and it has become increasingly important to systematically test, compare and possibly improve their accuracy as well as consistency.

The purpose of this work is twofold. First, for polymers with low polydispersity, our main goal is to check the consistency between published methods. Indeed, precise measurements on narrow disperse polymers are essential for testing the predictions of tube models in general. Residual discrepancies between definitive experimental data and theoretical predictions should help highlight shortcomings of the models. An important example of such a concern is the effect of finite chain-length on $G_{N\,\text{exp}}^0$. Significantly different predictions have been published by Kavassalis and Noolandi [32–34], Likhtman et al. [3] and Masubuchi et al. [35]. Those predictions should be confronted with unquestionable experimental data. Another important example concerns universal methods for relating polymer structure to macroscopic properties, including M_e and G_N^0 [36,37]. Fetters et al. has suggested that viscoelastic properties can be correlated with chain dimensions, in particular the packing length [21,38–40]. Again, definitive $G_{N\,\text{exp}}^0$ data are a prerequisite to test such approaches.

Our second objective is concerned with polydisperse polymers. As opposed to model systems, industrial polymers usually have broad polydispersity. Some systems (step condensation polymers for instance) cannot even be synthesized with polydispersity smaller than two. We, therefore, want to investigate the possible extension of methods for $G_{N\,\text{exp}}^0$ determination to polymer systems with broad distribution, in particular systems with polydispersity around two.

This paper is divided into six sections. In Section 2, we review the definition of entanglement spacing and discuss published methods for determining the plateau modulus of monodisperse polymers, as well as the assumptions and modifications necessary to adapt these methods to polydisperse systems. In Section 3, we describe the polymers used in this study, and include published experimental data as well as predictions from recent tube models. In Section 4, we assess the consistency and applicability of published methods by analyzing the dynamic moduli of monodisperse model polymers. We also briefly compare the observed molecular weight (MW) dependence of $G_{N\,\text{exp}}^0$ with theoretical predictions. In Section 5, modified methods for polydisperse polymers are analyzed and compared. Applications of the methods are illustrated by two important examples. Conclusions are presented in Section 6.

2. Theory and published methods

2.1. Definition of entanglement spacing and time

In tube models, the entanglement molecular weight M_e, defined as the average molecular weight between topological constraints, is the most fundamental material parameter, as envisioned by Edwards and de Gennes. M_e cannot be easily measured in a direct fashion and is usually inferred from a the plateau modulus G_N^0, which can be determined by measuring the dynamic moduli G' and G'' in oscillatory shear experiments:

$$G_N^0 = \frac{4}{5}\frac{\rho RT}{M_e}. \tag{1}$$

We follow the 'G definition' of the entanglement spacing [4], which means that the 'number of entanglements' per molecule, $Z = M/M_e$, is equal to the number of tube segments per molecule. On the other hand, M_e (or equivalently, the tube diameter a) also can be extracted from other experimental techniques [6], but those methods are restricted to a few polymer species [41], and the results need to be cross-checked with other techniques [42,43]. In present study, only the determination of G_N^0 by rheological methods is discussed.

Fig. 1 shows the master curve of the storage and loss moduli for a linear polybutadiene (PBD) with narrow molecular weight distribution (MWD) and very high MW (obtained from [44]). The characteristic times of different relaxation modes correlate with M_e via the number of entanglements Z as follows

$$\tau_R = Z^2 \tau_e, \tag{2}$$

$$\tau_d = 3Z^3 \tau_e, \tag{3}$$

where τ_R is the Rouse relaxation time of the chain, τ_e is the relaxation time of a segment between entanglements, and τ_d is the reptation disengagement time, uncorrected for contour length fluctuations (CLF).
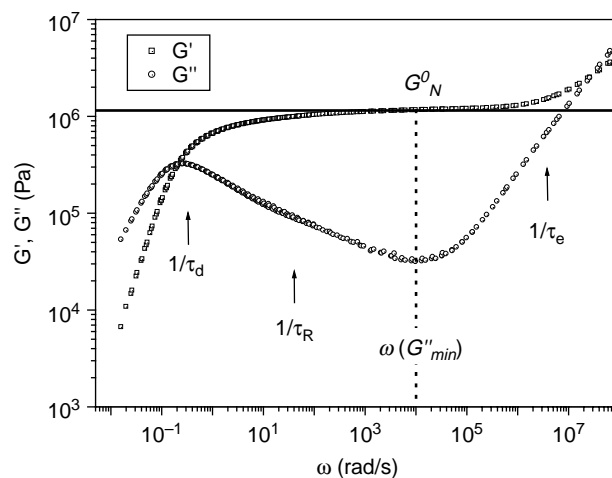

Fig. 1. Master curve of the storage and loss moduli for a monodisperse long chain polymer. Data for polybutadiene with $M_w = 410$ kg/mol and $Z \sim 260$ were obtained from Wang et al. [44].

2.2. Obtaining G_N^0 by fitting with tube models and associated problems

Eqs. (1)–(3) show that M_e influences both the modulus and the time scales of the viscoelastic response. Therefore, when all relevant relaxation processes are correctly treated, the basic modulus G_N^0 (and hence M_e) and the basic time τ_e should both be obtained by a theoretical fitting of the experimental data [3]. This is in principle the best method to obtain G_N^0. However, in the current state of the art, inconsistencies remain between the material parameters appearing in Eqs. (1)–(3), when the theoretical fitting procedure is used. There are at least three reasons for this.

First, there are still unavoidable approximations, even in the most sophisticated tube models developed so far. Archer et al. [45] recently indicated that independent fitting of the parameters G_N^0 and M_e (a violation of Eq. (1)) is necessary for all variants of the Milner–McLeish model [3,6,46,47], even for narrow distribution linear melts, which means current tube models need three basic parameters instead of two.

Second, no existing mixing-rule is fully satisfactory for polydisperse polymers [10,13,48]. This is due to the very complex nature of constraint release (CR) [5–7].

Third, a theoretical fitting of experimental data cannot eliminate experimental errors. Because information about MW and MWD is needed to predict relaxation times, the uncertainty about size exclusion chromatography (SEC) measurements will affect the predicted values of M_e as shown in Eqs. (2) and (3). Considering the worse reproducibility of SEC [49] as compared to rheology [50], uncertainties about the theoretical fitting for polydisperse polymers will presumably be larger than the experimental errors of the rheological measurements themselves.

Considering all the above factors, it is still very relevant to use semi-empirical methods for determining the plateau modulus. The results should in particular provide a reference for comparisons among variants of tube model.

2.3. Published methods for determining the plateau modulus of monodisperse polymers

Generally, $G_{N\,exp}^0$ can be determined by measuring linear viscoelastic (LVE) properties in oscillatory shear experiments (dynamic moduli). There are various semi-empirical methods to extract the value of $G_{N\,exp}^0$ from the LVE relaxation spectrum [17]. Fig. 1 clearly shows a quasi-plateau in the storage modulus vs. angular frequency curve, which is the famous signature of entanglements. However, although the G' plateau is essentially flat for exceedingly high MW and narrow-disperse polymers, there is no frequency at which a true plateau can be measured at finite molecular weight due to the overlap of different relaxation modes [5–7]. The convention is that the plateau modulus $G_{N\,exp}^0$ be determined from the value of G' at the frequency ω_{min} where G'' reaches a minimum [4,17]:

$$G_{N\,exp}^0 = G'(\omega)_{G''\to minimum}. \tag{4}$$

It is important to note that ω_{min} is close to the geometric mean of $1/\tau_R$ and $1/\tau_e$, and therefore, the Rouse modes and the terminal relaxation have similar contributions to G'' at that point. An accurate determination of $G_{N\,exp}^0$ by this method requires a wide separation of τ_R and τ_e and the corresponding relaxation modes. We call this approach the 'minimum' (MIN) method.

The second method [17,51] is derived from the Kronig–Kramers relation for G' and G''. It calculates $G_{N\,exp}^0$ by numerical integration over the terminal relaxation peak of $G''(\omega)$:

$$G_{N\,exp}^0 = \frac{2}{\pi} \int_{-\infty}^{+\infty} G''(\omega)\mathrm{d}\ln \omega. \tag{5}$$

This is called the 'integral' method (INT). The majority of the plateau modulus values reported in the literature have been obtained by this method [17,21,40]. Determination of the plateau modulus from Eq. (5) is unaffected by MWD, even though MWD alters the shape of the terminal relaxation. A key point for the INT method is that the terminal peak has to be correctly resolved from significant overlap with high-frequency Rouse modes. This complete separation of the terminal zone from the high frequency motions practically requires molecular weights of at least 50 times M_e.

The third method has been developed by Raju et al. [52]. It is based on an empirical 'universal' terminal spectrum inferred from observations on different monodisperse polymer species, as shown in Fig. 2. The universal shape can be rationalized from the predictions of tube models. For sufficiently narrow-disperse and long chains, the area under the loss modulus peak divided by the maximum of the G'' terminal peak should yield a universal proportionality constant K:

$$\frac{G_N^0}{G_{max}''} = 2.303 \left[\frac{2}{\pi} \int_{-\infty}^{+\infty} \frac{G''(\omega/\omega_{max})}{G_{max}''} \mathrm{d}\log(\omega/\omega_{max}) \right] = K. \tag{6}$$
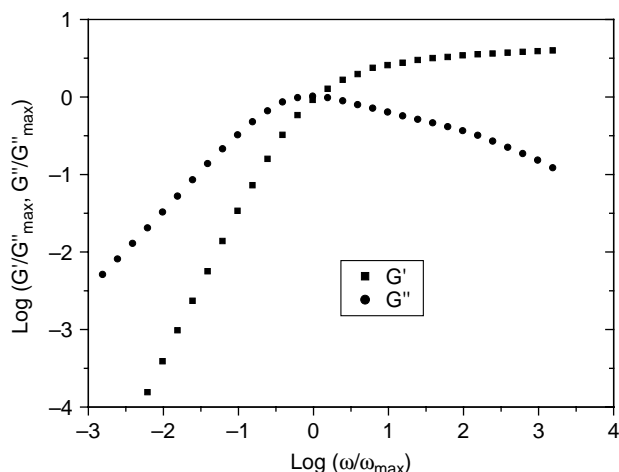

Fig. 2. Universal terminal relaxation spectrum for monodisperse polymers. Data were obtained from Raju et al. [52].

Raju et al. [52] have found $K = 3.56$. It is much easier to resolve the maximum of G'' ($Z \sim 20$) than the entire G'' terminal peak ($Z > 50$), since G''_{max} is rather unaffected by fluctuations and high frequency Rouse modes, which dominate the modulus at frequencies $\omega > \omega_{max}$. Because of its simplicity, this so-called 'maximum' method (MAX) has been used extensively for monodisperse polymer systems [38] and even for the high MW component in binary mixtures [53,44] as well as in solution [52,54]. However, Eq. (6) with $K = 3.56$, only applies to linear polymers with very narrow molecular weight distributions. Since, MWD alters the shape of the terminal relaxation, the value of K is a function of MWD, which will be discussed below.

2.4. Extension to polydisperse polymers

In principle, the best way to determine the plateau modulus G^0_N is to use narrow MWD and high MW samples, as discussed above. Unfortunately, most man-made polymers are polydisperse, and many polymer materials cannot even be synthesized with a polydispersity index close to 1. Therefore, methods validated for monodisperse model polymers must be extended to polydisperse systems. Since, the lowest achievable polydispersity for condensation polymers or metallocene polyolefins is around 2, this case is of particular interest.

A prerequisite for the valid extension of plateau modulus determination methods to polydisperse systems is that $G^0_{N \, exp}$ be independent from polydispersity. This question will be discussed and positively answered in Section 5.1, based on literature results.

Polydisperse polymers have intrinsically broader terminal relaxation spectra than monodisperse samples. Therefore, it is more difficult to correctly extract $G^0_{N \, exp}$. The influence of polydispersity on each of the three methods discussed earlier is presented below.

2.4.1. MIN method
The visual G' plateau becomes severely frequency-dependent due to the width of the relaxation spectrum. The slope of G' in the plateau region increases with increasing polydispersity. On the other hand, the negative slope of G'' at the high-frequency side of the terminal peak is decreasing, leaving ω_{min} indistinct. Hence, at the same time, ω_{min} is poorly defined and the influence of this uncertainty on the corresponding G' is large. In some systems with very broad MWD or low MW, G'' does not have a minimum and a maximum. Only $\tan \delta = G''/G'$ has a minimum as shown in Fig. 3. Therefore, a modification of the MIN method has been suggested by Wu [28,55,56].

$$G^0_{N \, exp} = G'(\omega)_{\tan \delta \to minimum}.$$ (7)

However, Eq. (7) is rather arbitrary. Lomellini [57] has discussed this method in detail.

2.4.2. INT method
For polydisperse polymers, it is more difficult to completely separate the terminal zone from the high frequency Rouse
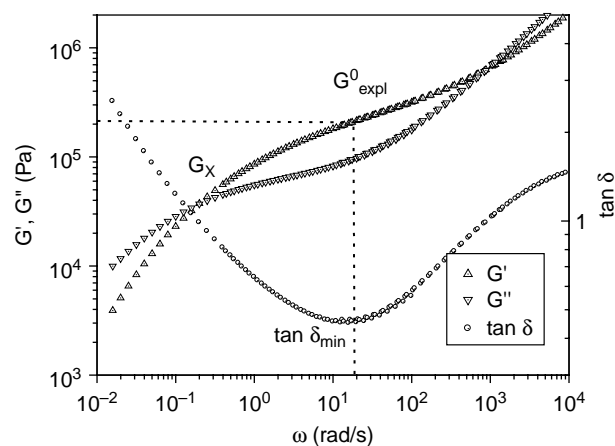

Fig. 3. Master curve of the storage and loss moduli for a polydisperse polymer. Data for polyisobutylene (PIB-15) with $M_v = 85$ kg/mol ($M_v/M_e \sim 15$) and $M_v/M_n = 2$; M_v is viscosity average MW.

relaxation because the terminal relaxation of the low MW components overlap with the high-frequency Rouse modes. Since, the terminal relaxation spectrum is broad for polydisperse systems, some authors have argued that the loss modulus peak should be reasonably symmetric. Therefore, the INT method can be simplified by taking twice the area of the peak up to the frequency of the maximum, thereby avoiding integration over the problematic high-frequency region [8,58]:

$$G^0_{N \, exp} = \frac{4}{\pi} \int_{-\infty}^{\omega_{max}} G''(\omega) d\ln \omega.$$ (8)

Eq. (8) unfortunately gives a $G^0_{N \, exp}$ value that is a systematically smaller than the one calculated from Eq. (5) because the true terminal peak is always skewed toward high frequencies (this is an essential consequence of CLF and CR). Eq. (8) can be used as a replacement in some cases when there are not enough experimental data at high frequencies, or as a supplement and confirmation of the results obtained by Eq. (5) (keeping in mind it only gives a lower bound).

2.4.3. MAX method
A modified MAX method has been proposed by Marvin–Oser [59]:

$$G^0_{N \, exp} = 4.83 G''_{max}.$$ (9)

This old equation is based on a shifted Rouse model for the terminal spectrum of uniform entanglement spacing [17], which is very remote from what we now consider the true dynamics of entangled polymers. The observed agreement with experiments (in particular for polymers with polydispersity close to 2), therefore, appears as a mere coincidence.

2.4.4. Crossover modulus-based methods
For polymers with low MW and high MWD, the minimum and maximum of G'' can become indistinct. Moreover, semi-crystalline polymers have a very limited dynamic window since they can only be measured far above the glass transition.

In these cases, Eqs. (7)–(9) may not work. Alternative methods based on the terminal crosspoint of G' and G'' ($G_x = G' = G''$ at angular frequency $\omega = \omega_x$) have been proposed by Wu [28] and Nobile–Cocchini [11]. The Wu method correlates the ratio between the crossover modulus and the plateau modulus to the polydispersity

$$\log\left(\frac{G_N^0}{G_x}\right) = 0.38 + \frac{2.63\log\frac{M_w}{M_n}}{1 + 2.45\log\frac{M_w}{M_n}}, \tag{10}$$

where G_x is the crossover modulus and M_w/M_n should be less than about 3. The M_z/M_n ratio was added to the formula by Nobile–Cocchini for improved accuracy:

$$\log\left(\frac{G_x}{G_N^0}\right) = \frac{-0.524 + 0.341\log\frac{M_w}{M_n} - 1.843\log\frac{M_z}{M_w}}{1 - 0.559\log\frac{M_w}{M_z} + 0.841\log\frac{M_z}{M_w}}. \tag{11}$$

Obviously, the plateau modulus values obtained from Eqs. (10) and (11) are tentative due to the approximations embedded in the relationships.

3. Tested systems and models

3.1. Experimental data for monodisperse model polymers

The most recent studies on monodisperse model polymers are concerned with polybutadiene (PBD), polyisoprene (PI), and polystyrene (PS), which can be synthesized with widely different molecular weights and nearly monodisperse distribution by anionic polymerization techniques. Since, the plateau modulus can be affected by microstructure, we limit ourselves in this paper to published results for 1,4-polybutadiene with ∼50/40/10 of trans/cis/vinyl units and 1,4-polyisoprene with ∼75/20/5 of trans/cis/3,4 units [21]. The plateau moduli and molecular characteristics of the selected samples are listed in Tables 1–3 for PBD [44,52,53,60–62], PI [63–69] and PS [57,58,70,71]. In addition, a set of rheological data for PBD with different MW [44] has been kindly supplied by Prof. Wang. Those are frequently used in Section 4.

3.2. Experimental data for polydisperse polymers

Polydisperse polymers include commercial polymers and mixtures of monodisperse polymers. The rheological data on binary mixtures of monodisperse PBD have been kindly supplied Prof. Wang and are summarized in Table 4. Commercial polyisobutylene (PIB) samples with broad MWD, Oppanol B 15, B 50 and B 150, have been kindly supplied by BASF AG (Dr Laun). Rheological measurements on PIB were made over a wide range of temperatures from −40 to 200 at about 30 °C intervals. All corresponding data are listed in Table 5. The plateau moduli and molecular characteristics of Ethylene–Octene copolymers (EOC) [72] have been kindly supplied by Exxon-Mobil Chemical (Dr Garcia-Franco). They are reported in Table 7. Plateau

Table 1
Monodisperse PBD samples: plateau moduli $G_{N\ exp}^0$ (MPa) estimated by different methods and molecular characteristics

Sample[a]	$G_{N\ exp}^0$ [b]	$G_{N\ exp}^0$ [c]	$G_{N\ exp}^0$ [d]	G_{max}''	M_w (kg/mol)	M_w/M_n	Temperature (°C)	Ref.
44K	1.20	1.17 (1.33)[e]	1.19	0.333	43.8	1.01	40	[44]
100K	1.18	1.13	1.15	0.323	99.1	1.01		
207K	1.15	1.15	1.25	0.352	208	1.01		
410K	1.15	1.10	1.15	0.323	412	1.01		
L200			1.15	0.323	200	<1.05	25	[52]
L350			1.18	0.331	350	<1.05		
41L			1.05	0.305	40.7	1.04	25	[53]
98L			1.23	0.345	97.5	1.03		
174L			1.21	0.34	174	1.04		
435L			1.23	0.345	435	1.03		
B1			1.12	0.314	70.9	<1.05	25	[60,61]
B2			1.09	0.307	130	<1.05		
B3			1.20	0.337	355	<1.05		
B4	∼1.1$_5$[f]	1.15	1.26	0.355	925	<1.05		
PBD21	-	1.10	1.26	0.354	20.7	<1.1	28	[62]
PBD41	1.10	1.08	1.24	0.349	44.1	<1.1		
PBD97	1.09	1.12	1.22	0.343	97	<1.1		
PBD201	1.20	1.15	1.27	0.356	201	1.27		
Average	1.15±0.05	1.13±0.03	1.18±0.07	0.33±0.02				

[a] Codes in original references.
[b] Estimated by using 'MIN' method of Eq. (4).
[c] Estimated by using 'INT' method of Eq. (5).
[d] Estimated by using 'MAX' method of Eq. (6).
[e] 'INT' method by direct extrapolating G'' at the high frequency.
[f] G' value at the highest attainable frequency [61].

Table 2
Monodisperse PI samples: plateau moduli $G_{N\,exp}^0$ (MPa) estimated by different methods and molecular characteristics

Sample[a]	$G_{N\,exp}^0$ [b]	$G_{N\,exp}^0$ [c]	$G_{N\,exp}^0$ [d]	G_{max}''	M_w (kg/mol)	M_w/M_n	Temperature (°C)	Ref.
PI-0.634L			0.356	0.1	76.5	1.03	25	[63]
PI-0.729L			0.342	0.096	86.1	1.03		
PI-0.920L			0.375	0.105	105	1.03		
PI-0.922L			0.354	0.099	108	1.04		
PI-0.991L			0.344	0.097	132	1.04		
PI-1.115L			0.333	0.094	164	1.05		
PI-1.596L			0.363	0.102	233	1.03		
		0.36			504		−10	[64]
L49	0.332	-	0.409	0.115	48.8	1.05	40	[65–68]
L94	0.433	0.429	0.402	0.113	94.0	1.05		
L180	0.402	0.416	0.392	0.110	180	1.06		
L308	0.467	0.434	0.399	0.112	308	1.08		
			BSW[e]	Ne[e]			25	[69]
PI80K			0.43	0.22	75	1.06		
PI100K			0.42	0.19	102	1.04		
PI163K			0.32	0.17	110	1.02		
PI140K			0.38	0.26	128	1.08		
PI190K			0.39	0.19	198	1.03		
PI300K			0.38	0.23	293	1.02		
PI463K			0.38	0.23	464	1.05		
PI570K			0.35	0.23	576	1.09		
PI730K			0.35	0.21	735	1.04		
PI930K			0.37	0.22	963	1.12		
PI1000K			0.37	0.24	1013	1.05		

[a] Codes in original references.
[b] Estimated by using 'MIN' method of Eq. (4).
[c] Estimated by using 'INT' method of Eq. (5).
[d] Estimated by using 'MAX' method of Eq. (6).
[e] Estimated by using BSW fit, Ne is the slope on the right side of G_{max}''.

modulus data of polydisperse polyethylene (PE) [17–26] and for bisphenol-A polycarbonate (PC) [21,27–31] have been taken from the literature. All rheological parameters and molecular characteristics are listed in Tables 8 and 9. Measurements on linear PC (A-2700, supplied by Idemitsu Petrochemical Co. [73]) were performed at temperatures ranging from 160 to 210 °C with 20 °C intervals. For maximal accuracy, care was taken to calibrate the rheometer according to recommended procedures as well as load and trim the samples in the most reproducible manner possible [74]. We also took care to avoid transducer compliance problems, which cause large measurement errors when sample stiffness

Table 3
Monodisperse PS samples: plateau moduli $G_{N\,exp}^0$ (10^5 Pa) estimated by different methods and molecular characteristics

Sample[a]	$G_{N\,exp}^0$ [b]	$G_{N\,exp}^0$ [c]	$G_{N\,exp}^0$ [d]	G_{max}''	M_w (kg/mol)	M_w/M_n	Temperature (°C)	Ref.
L15		1.9			215	1.00	160	[58]
L22		1.8			275	1.07		
L19		2.22			513	1.09		
L18		2.05			581	1.06		
PS100f2			1.83	5.15	115		169.5	[70]
C6bb		2.06	1.78	5.01	275			
C7bb		2.11	1.78	5.01	860			
290			1.85	5.20	290		180	[71]
750			1.80	5.06	750			
2540			1.85	5.20	2540			
PS-3	2.06				222	1.04	150	[57]
PS-2	2.09				327	1.03		
PS-1	2.06				756	1.03		

[a] Codes in original references.
[b] Estimated by using 'MIN' method of Eq. (4).
[c] Estimated by using 'INT' method of Eq. (5).
[d] Estimated by using 'MAX' method of Eq. (6).

Table 4
Integration of G'' for the binary mixtures of PBD 410 K and PBD 100 K at 40 °C [44]

ϕ_L	$G_{N\,\exp}^0$ (MPa)
1	1.10
0.8	1.11
0.6	1.08
0.4	1.14
0.2	1.12
0.1	1.07
0.05	1.13
0	1.13

approaches the spring constant of the transducer. For this reason, 8 mm parallel plates were used for PIB and the PC samples.

3.3. Theoretical predictions of tube models

Recent tube models can generate quantitative predictions of linear viscoelasticity (LVE) and make it possible to systematically analyze the effect of polydispersity. We have obtained predictions of LVE by two recently published tube models, for polymers with polydispersity comprised between 1.0 and 5.0.

For monodisperse polymers, we use the predictions of the Likhtman–McLeish quantitative theory [3]. Predicted normalized LVE spectra are available on Dr Likhtman's web-page [3] for Z ranging from 2 to 1000. Following the authors' suggestion, predictions with the constraint release (CR) parameter $c_v = 1$ were used for comparison with experimental data.

For polydisperse systems, we use the model published by van Ruymbeke et al. [13,31]. The MWDs are represented by generalized exponential functions (GEX) [11] with $Z = 200$, and the polydispersity is varied from 1.01 to 5 (Table 6). The terminal relaxation spectra (without inclusion of high frequency Rouse modes) are calculated using the MWD inputs according to the procedure and parameters described in Ref. [13,31].

4. Results for monodisperse model polymers

4.1. Consistency of published methods

4.1.1. Controlled set of PBD data

In order to check different methods for the determination of $G_{N\,\exp}^0$, we first use a set of accurate LVE data for linear

PBD published by Wang et al. [44] and presented in Fig. 4(a) and (b). The quality of the data is reflected by the very narrow distribution of the samples (polydispersity about 1.01), the wide range of M_w's (from 44 to 410 kg/mol), the excellent superposition of the high-frequency Rouse relaxation, and the similar WLF frequency–temperature shift factors a_T for the different samples. On the master curves, the terminal zone progressively shifts to low frequencies and the visual G' plateau widens as MW increases. We first use the MIN method, according to Eq. (4). For high MW samples, the results are accurate but for the lowest MW sample, there is a big uncertainty due to the increasing slope in the plateau region. Next, we use the INT method according to Eq. (5). For low MW samples PBD 44k, it is necessary to subtract the contribution of the high frequency Rouse relaxation. This procedure will be discussed in detail in Section 4.2. Finally, we can use the MAX method by directly reading the values of $G''_{\max}$ and converting them to $G_{N\,\exp}^0$ according to Eq. (6). All $G_{N\,\exp}^0$ values obtained with the different methods are listed in Table 1 for the four PBD samples.

The three methods agree with each other within an uncertainty of 5%, which demonstrates their consistency.

4.1.2. Data for different polymers and from different sources

With the knowledge that all three methods give consistent results for a controlled set of samples of a single polymer, we next assess the situation for a broader range of MW and for other polymers. Therefore, we reanalyze published rheology data for monodisperse PBD, PI and PS with a wide range of MW and from different sources. All the collected MW information and the recalculated $G_{N\,\exp}^0$ values according to the three methods described above are listed in Tables 1–3, respectively. In the PBD case, the M_w range is from 20 kg/mol to about 1000 kg/mol (corresponding to $Z \sim 10$–600), and all $G_{N\,\exp}^0$ values are located between 1.05 and 1.27 MPa. The average value from the MIN method is 1.15 ± 0.05 MPa while the average from the INT method is 1.13 ± 0.03 MPa and the average from the MAX method is 1.18 ± 0.07 MPa. The combined average of all data is 1.16 ± 0.06 MPa, which agrees very well with the value of 1.15 MPa obtained for the highest M_w sample (PBD-925K) reported by Colby et al. [61], using the INT method. All $G_{N\,\exp}^0$ results are plotted as a function of MW and Z in Fig. 5. The entanglement molecular weight M_e, calculated from Eq. (1), is 1570 g/mol for PBD ($\rho = 896$ kg/m^3 at 25 °C [21]). Clearly, the three methods are very consistent and give values that agree within an uncertainty of about 5% for each sample, which is comparable with experimental errors due to sample loading [7,74,75].

Table 5
Polydisperse PIB samples: plateau moduli $G_{N\,\exp}^0$ (10^5 Pa) estimated by different methods at 25 °C and molecular characteristics

Sample	Eq. (4)	Eq. (7)	Eq. (5)	Eq. (8)	$G''_{\max}$	Eq. (5)/$G''_{\max}$	G_x	Eq. (10)	M_v (kg/mol)[a]	M_n (kg/mol)[a]	M_v/M_n[a]	M_v/M_e (M_n/M_e)
B150	3.12	3.14	3.18	2.48	0.478	6.66	0.314	3.84	2600	425	6.12	456 (75)
B50	2.80	2.93	3.20	2.72	0.517	6.18	0.326	3.13	400	120	3.33	70 (21)
B15	–	2.15	2.90	2.66	0.539	5.38	0.365	2.59	85	40.8	2.08	15 (7.2)

[a] From supplier.

Table 6
G_N^0/G_{max}'' and G_N^0/G_x as a function of M_w/M_n from theoretical predictions and empirical relationships for long chain with $Z=200$

M_w/M_n	G_N^0/G_{max}'' [a]	G_N^0/G_x [a]	G_N^0/G_x [b]	G_N^0/G_x [c]
1.01	3.5	3.5	2.5	2.2
1.03	3.6	3.6	2.6	2.3
1.07	3.7	3.8	2.8	2.4
1.1	3.9	4.0	3.0	2.5
1.2	4.2	4.4	3.6	2.8
1.3	4.4	4.9	4.1	3.2
1.5	4.8	5.8	5.0	3.9
1.7	5.2	6.7	5.8	4.6
2	5.5	7.9	6.8	5.8
3	6.5	11.8	9.1	9.6
4	7.0	15.2	10.5	13.3
5	7.5	18.5	11.4	17.0

[a] Tube theoretical predictions.
[b] Wu relationships of Eq. (10).
[c] Nobile–Cocchini relationships of Eq. (11), and the M_z/M_w ratio has been fixed at 0.75 M_w/M_n (see EOC case in Table 7).

G_N^0 exp values are also plotted as a function of MW and Z in Figs. 6 and 7 for PI and PS, respectively. In the PI case, MW ranges from 49 to about 1000 kg/mol ($Z \sim 10$–200), and the combined average for G_N^0 exp value is 0.38 ± 0.04 MPa (including data obtained by using the empirical BSW fit [76] in Ref. [69]). In the PS case, MW ranges from 115 kg/mol to about 2500 kg/mol ($Z \sim 7$–180), and the average G_N^0 exp is 0.195 ± 0.015 MPa when using all data. The entanglement molecular weight M_e calculated from Eq. (1) is 4730 g/mol for PI ($\rho=900$ kg/m^3 at 25 °C) [21], and 14,800 g/mol for PS ($\rho=959$ kg/m^3 at 210 °C [39]). Examination of Figs. 6 and 7 reveals the same level of consistency for PI and PS as for PBD.

We can conclude that for well-entangled linear model polymers with low polydispersity ($M_w/M_n < 1.1$ and $Z > 20$), such as polybutadiene, polyisoprene and polystyrene, results for the experimental plateau modulus extracted by the three methods show satisfying agreement within 10%. The uncertainty generated by the data reduction methods is not higher than the experimental error of the LVE measurements themselves. In other words, the different methods are consistent from the experimental point of view.

From Figs. 5–7, another important conclusion can be drawn. The observed MW or Z dependence of G_N^0 exp or of G_{max}'' is very weak and certainly lower than the predictions (G_N^0 exp $\sim Z^{0.1-0.15}$) by CLF-dominated tube models [3,4,46,77], as shown in Fig. 8. A significant implication of the discrepancy between the experimental results and theoretical predictions is the overestimation of CLF effects by advanced tube models. This is discussed in a separate paper [78].

4.2. Universal terminal relaxation spectra and subtraction of the high-frequency Rouse contribution

The concept of a universal relaxation spectrum in the terminal zone was first proposed on experimental grounds from the analysis of different monodisperse polymer species by Raju et al. [52]. It is also consistent with predictions of the tube model for highly entangled polymers ($Z \gg 1$) where CLF and CR do not influence the shape significantly, in particular at frequencies up to ω_{max} [3,5–7]. Fig. 9 shows the experimental G'' terminal peak for a high MW PBD sample ($MW=410$ kg/mol, $Z=262$) as well as theoretical predictions by a state-of-the-art tube model [3] for the corresponding number of entanglements and the correspondence with the empirical universal terminal spectrum proposed by Raju et al. [52]. All three curves have been scaled by G_{max}'' vertically and ω_{max} horizontally for easier comparison. The experiments and theoretical predictions by the Likhtman–McLeish theory agree very well for this highly entangled linear chain. Similarly, if we forget about the high frequency Rouse relaxation, the terminal relaxation is well captured by the universal terminal spectrum.

Mainly as a consequence of relaxation by CLF and CR, the slope of the loss modulus curve for a monodisperse polymer at $\omega > \omega_{max}$ is close to $-1/4$ [3,5–7,46]. A similar slope of -0.23 is obtained by applying the empirical BSW spectrum [69,76,79]. For high MW samples, when the terminal peak and Rouse region are well separated (Fig. 9), this slope can be conveniently extended at high frequency in the Rouse-dominated region to provide a reasonable extrapolation of the terminal peak.

Table 7
Polydisperse ethylene–octene copolymers (EOCs) samples: plateau moduli G_N^0 exp (MPa) estimated by different methods at 190 °C and molecular characteristics [72]

Sample[a]	C8 mol %	G_N^0 exp [b]	G_{max}''	G_N^0 exp [c]	G_{expl}^0/G_{max}'' [b]	G_x	G_N^0 exp [d]	G_N^0 exp [e]	M_w (kg/mol)	M_w/M_n	M_z/M_w
EO30	9.6	1.27	0.296	1.43	4.29	0.149	1.00	0.84	129	1.95	1.48
EO38	13.0	0.81	0.189	0.91	4.26	0.125	0.85	0.70	173	1.99	1.47
EO44	16.2	0.79	0.158	0.76	4.98	0.090	0.62	0.52	197	2.01	1.51
EO52	21.6	0.57	0.119	0.57	4.80	0.072	0.50	0.42	233	2.01	1.50
EO56	24.3	0.46	0.093	0.45	5.00	0.056	0.40	0.32	285	2.10	1.48
EO70	37.2	0.25	0.049	0.24	5.03	0.035	0.23	0.18	941	1.95	1.39
EO87	63.4	0.13	0.025	0.12	5.07	0.018	0.12	0.090	1270	1.96	1.36
EO92	75.1	0.090	0.020	0.096	4.53	0.012	0.084	0.063	1080	1.94	1.37

[a] Codes in original references.
[b] Estimated by using 'INT' method of Eq. (5).
[c] Estimated by using 'MAX' method of Eq. (9).
[d] Estimated by using Wu relationships of Eq. (10).
[e] Estimated by using Nobile–Cocchini relationships of Eq. (11).

Table 8
Polydisperse PE samples: plateau moduli $G_{N\,exp}^0$ (MPa) estimated by different methods and molecular characteristics

Sample[a]	$G_{N\,exp}^0$ [b]	$G_{N\,exp}^0$ [c]	$G_{N\,exp}^0$ [d]	M_w (kg/mol)	M_w/M_n	Temperature (°C)	Ref.
SNPA-5[e]		1.58	1.5 (0.42)	265	1.12	190	[18]
PHPB-4		2.73		187		190	[19]
PHPB-5		2.08		244			
EHPB-2		2.35		194			
HPB-3		2.58		211	1.05		
HPB-4		1.83		360	1.05		
Average		2.31					
HDPE		2.3					[17]
HPB		2.7[f]			$-b_T$	100	[20,21]
HDL4	1.8	1.9	1.88 (0.39)	329	2.08	150	[22]
PEL125		2.45		127	1.01	190	[23]
PEL147		1.97		148	1.01		
PEL193		1.79		195	1.01		
PEL243		1.75		255	1.05		
PEL280		1.86		290	1.02		
PEL689		2.00		789	1.15		
Average		1.97					
PE800	1.92	2.07	2.51 (0.52)	800	1.8	160	[26]
PE3600	1.95			3600	2.9	160	
mPEL2		1.01		152	2.3		[24]
mPEL3		1.00		170	2.2		[25]
mPEL4		1.03		173	2.1		
mPEL5		1.09	1.21 (0.25)	185	2.2		

[a] Codes in original references.
[b] Estimated by using 'MIN' method of Eq. (7).
[c] Estimated by using 'INT' method of Eq. (5).
[d] Estimated by using 'MAX' method of Eq. (9), the value in parentheses for G''_{max}.
[e] Fraction sample.
[f] Extrapolation to zero vinyl content.

For low-*MW* samples, the direct extrapolation described above becomes inaccurate and another procedure is preferred: subtracting the 'Rouse' contribution from the loss modulus curve in order to obtain a corrected terminal peak. For high-*MW* samples (as shown in Fig. 9), the terminal and Rouse relaxations are completely separated. Hence, the 'Rouse slope' for G'' above ω_{min} can easily be determined. The observed slope can be different from the 0.5 value predicted by the Rouse model [6,17,60,79,80]. In Fig. 9 the measured slope is about 0.71 for PBD. In the present paper, we use the experimental 'Rouse slope' obtained from high-*MW* samples to determine the *MW*-independent high frequency Rouse contribution to G'', also for low *MW* samples. Figs. 10 and 11 show the corrected experimental peaks as well as the universal spectrum (with frequency scale normalized by ω_{max}) for a 44 kg/mol and a 100 kg/mol PBD, respectively. A direct extrapolation of the terminal peak for the 44 kg/mol sample would yield $G_{N\,exp}^0 = 1.33$ MPa (in parentheses of Table 1) by the INT method, which is unreasonably high, compared with a value of 1.17 MPa obtained after the subtraction of Rouse modes.

Table 9
Polydisperse PC samples: plateau moduli $G_{N\,exp}^0$ (MPa) estimated by different methods and molecular characteristics

Sample[a]	$G_{N\,exp}^0$ [b]	$G_{N\,exp}^0$ [c]	$G_{N\,exp}^0$ [d]	M_w (kg/mol)	M_w/M_n	Temperature (°C)	Ref.
Mw40	1.83–1.96[e]			40		150	[27]
Mw90	1.60–1.71			90			
PC	2.2			48	2.2	200	[28]
CD 2000	2.0			33	2.6	190	[29]
PC			4.07[f]	150	2.4	170	[30]
PC			1.2[g]	39	1.4	200	[31]
PC		2.7	2.7–11.2[h]			200	[21]
A-2700	2.17	2.29	2.32 (0.48)	35	2.1	180	Idemitsu, 8 mm

[a] Codes in original references.
[b] Estimated by using 'MIN' method of Eq. (7).
[c] Estimated by using 'INT' method of Eq. (5).
[d] Estimated by using 'MAX' method of Eq. (9), the value in parentheses for G''_{max}.
[e] Tensile stress relaxation–inflexion of $3G_2$.
[f] BSW fitting.
[g] Tube model fitting.
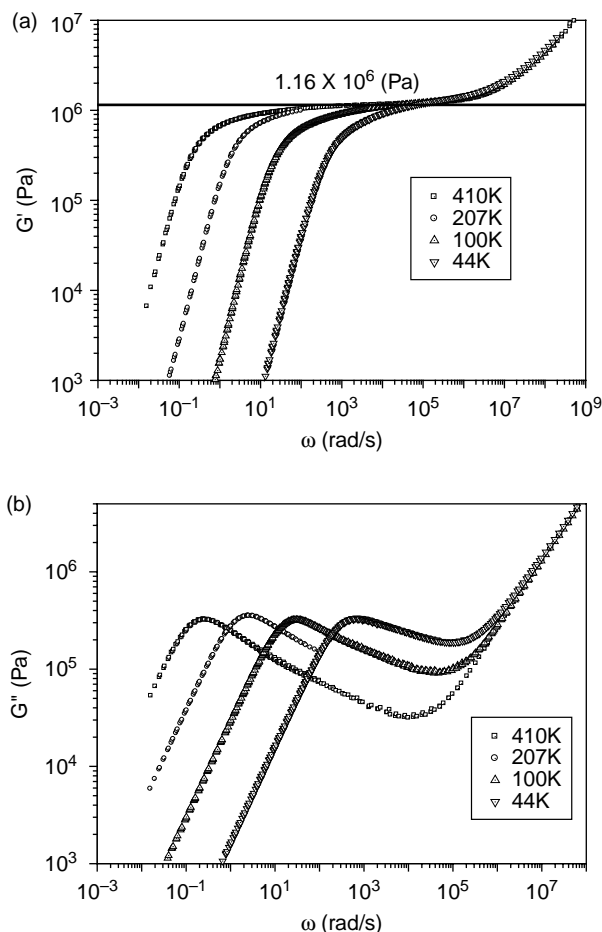[h] Rotational isomeric state (RIS) calculations.

Fig. 4. Master curves for (a) the storage moduli G' and (b) the loss moduli G'' of four monodisperse PBD samples at 40 °C. Data were obtained from Wang et al. [44].

Examination of Figs. 9–11 indicates that the universal peak is very close to the experimental corrected peak for Z around 60. On the low frequency side, no significant differences are observed between different MW samples, while, on the high
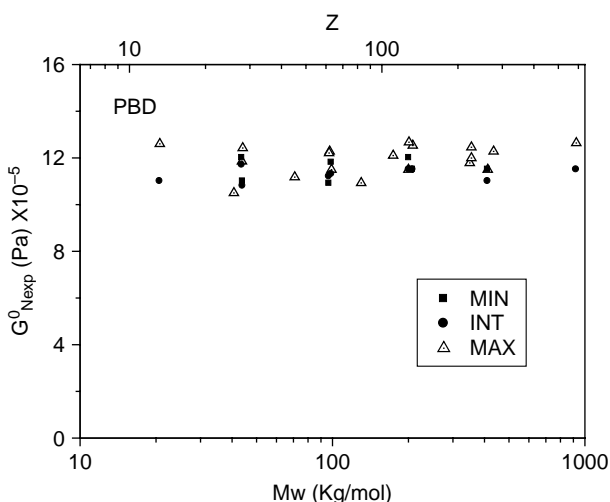

Fig. 6. $G_{N\,\text{exp}}^0$ values obtained by different methods as a function of M_w and Z for PI. References and discussions in the text.

frequency side, the experimental peak is slightly broader for lower Z and narrower for higher Z.

4.3. Applicability and accuracy of published methods

The MIN method is only accurate for highly entangled polymers. For low MW samples, fast Rouse relaxation processes will interfere with a terminal peak, itself broadened by CLF and CR effects. The widening of the terminal peak should cause an underestimation of G_N^0. On the other hand, overlap with Rouse relaxation should cause an overestimation of G_N^0. For PS, the two effects compensate each other exactly and give a constant value for G' at the frequency where $\tan \delta$ reaches a minimum, for Z between 2 and 50 [57]. This exact compensation for low MW samples should be seen as a mere coincidence. On the other hand, when transducer compliance or phase angle problems become severe (high G_N^0 polymers and/or high frequency measurements) the determination of

Fig. 5. $G_{N\,\text{exp}}^0$ values obtained by different methods as a function of M_w and Z for PBD. References and discussions in the text.
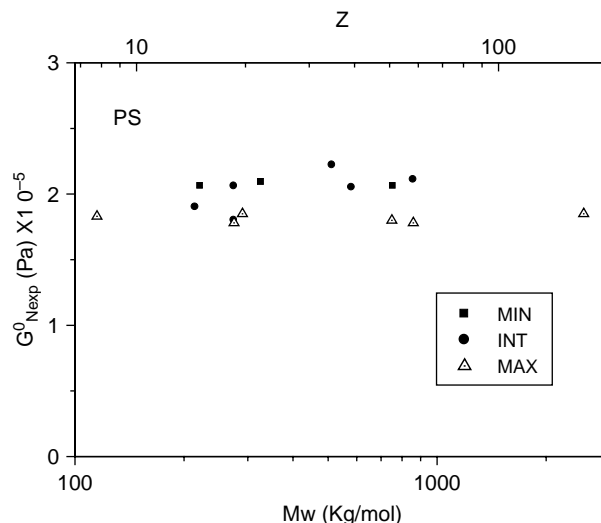
Fig. 7. $G_{N\,\text{exp}}^0$ values obtained by different methods as a function of M_w and Z for PS. References and discussions in the text.
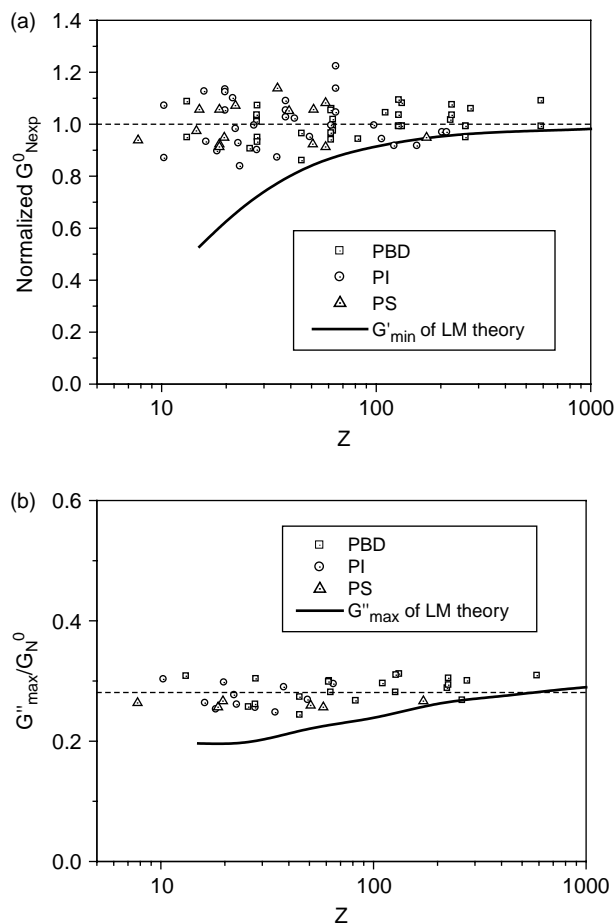
Fig. 8. (a) Dependence of $G_N^0{}_{exp}$ on Z: experimental data vs. theoretical predictions [3]. (b) Dependence of G''_{max} on Z: experimental data vs. theoretical predictions. Experimental data were normalized by $G_N^0 = 1.16$, 0.38, and 0.195 MPa for PBD, PI, and PS, respectively. Data were obtained from Figs. 5–7.

ω_{min} becomes inaccurate. This generates a big error for low MW samples, due to the steep slope in the plateau region. For these reasons, the use of the MIN method should be restricted to polymers with Z above 30, as shown in Table 1 and Fig. 8(a).

For the INT method, a complete separation of the terminal zone from the higher frequency Rouse relaxation practically requires $Z > 50$–60. The disturbance of Rouse modes can be removed by the Rouse subtraction procedure described earlier, but a necessary condition is that the high-frequency Rouse region be well measured and defined.

It is probably most convenient and accurate to get $G_N^0{}_{exp}$ values by the MAX method for monodisperse samples. However, strictly speaking, the G'' terminal relaxation spectrum is not completely universal. First, G''_{max} should have a very weak Z-dependence due to CLF effects [3], although, as shown Fig. 8(b), the experimentally observed dependence is vanishingly small [78]. Second, the shape of the terminal relaxation peak (at the high frequency side) is Z dependent at low Z and even possibly polymer-dependent [52,54,81–83]. Therefore, it can be argued that the constant K in Eq. (6) is not completely universal.

In summary, we have assessed three methods corresponding to Eqs. (4)–(6) for the determination of the

experimental plateau modulus. For the long-chain model polymers ($M_w/M_n < 1.1$ and $Z > 20$–30), there is satisfactory agreement within 5–10% between the various methods. The so-called universal terminal relaxation has also been validated for long chains. The strong dependence of $G_N^0{}_{exp}$ or G''_{max} on molecular weight as $Z^{0.1-0.15}$, predicted by the LM theory [3,4,77], is not observed experimentally in the Z range 10–600 for narrow-distribution samples.

5. Results for polydisperse polymers

Since, many synthetic polymers have intrinsically high polydispersity, there is a strong need to extend methods validated by monodisperse model polymers to polydisperse systems. Polydispersity causes a big uncertainty about G_N^0, especially for many condensation polymers and semicrystalline polyolefins, since high MW and/or narrow MWD samples are difficult to obtain. For example, published $G_N^0{}_{exp}$ values for
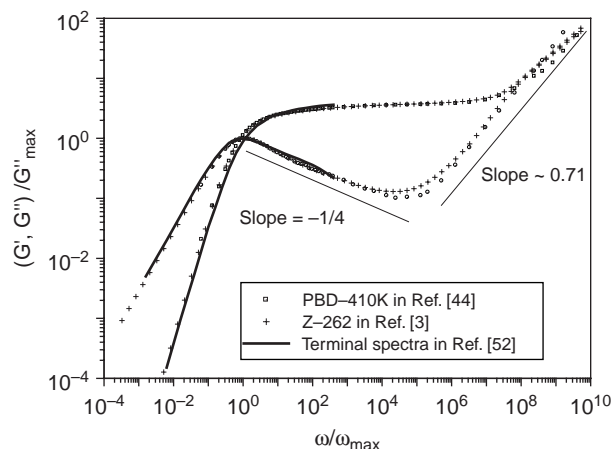

Fig. 9. Experimental curves for monodisperse PBD-410K [44] with $M_w = 410$ kg/mol ($Z = 262$) are compared to theoretical predictions with $Z = 262$ for the LM model [3], and the universal relaxation spectrum [52]. All three curves have been scaled by G''_{max} vertically and ω_{max} horizontally.
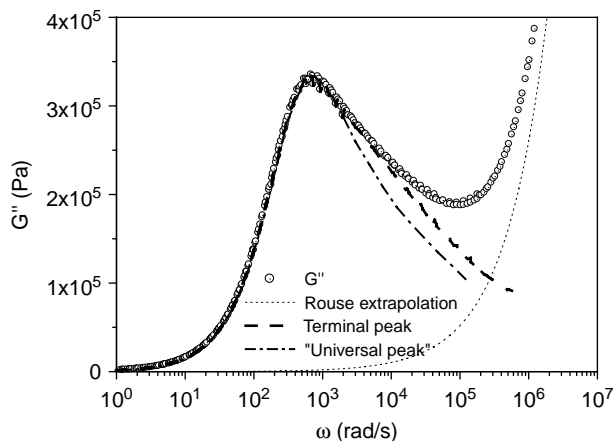

Fig. 10. Subtraction of 'Rouse' modes from the terminal peak for PBD 44K. The dotted line with slope ~ 0.71 is the extrapolation of the 'Rouse' relaxation; the dashed line represents the pure terminal relaxation peak. The dash–dot line represents universal the terminal peak.
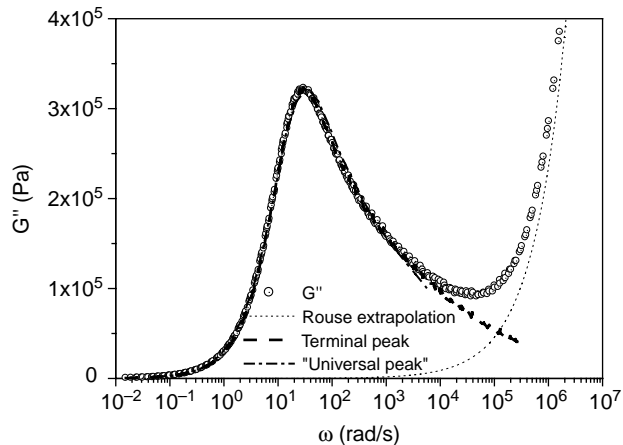
Fig. 11. Subtraction of 'Rouse' modes from the terminal peak for PBD 100 K. The dotted line with slope ~ 0.71 is the extrapolation of the 'Rouse' relaxation; the dashed line represents the pure terminal relaxation peak. The dash–dotted line represents the universal terminal peak.

semi-crystalline PE range from 1.1 up to 2.6 MPa [17–26], while for PC, $G_{N\ exp}^0$ values are scattered between 1.2 and 4.1 MPa [21,27–31]. Therefore, two questions arise:

(i) Does polydispersity influence the plateau modulus G_N^0 and hence the entanglement molecular M_e?
(ii) If not, how does it influence the determination of $G_{N\ exp}^0$?

These questions are answered in the next two subsections. A third subsection on significant practical examples completes the section.

5.1. Does polydispersity influence the plateau modulus?

The tube model suggests that M_e is independent of MW and MWD above a critical molecular weight (not higher than a few times M_e). It has also been reported, [30,53,84,85] that G_N^0 is experimentally independent of polydispersity, which is clearly illustrated by the results for bimodal blends of monodisperse PBD ($Z = 262$ and 63) shown in Fig. 12 (obtained from the Ref. [44]). The storage modulus shows an inflection between the frequencies of the two G'' maxima, corresponding to the terminal relaxation of the long and short chains, respectively. Above the second G''_{max}, G' approaches the plateau modulus of the pure components, demonstrating that G_N^0 is indeed independent of polydispersity. On the other hand, as seen in Fig. 12(b), the distance between the two relaxation maxima is reduced due to CR effects speeding up relaxation of the long chains and slowing down relaxation of the short ones (see for instance [53] and [86]). Numerical integration of the whole G'' terminal zone (using the previously described extrapolation at the high-frequency side) yields $G_{N\ exp}^0$ values for the pure components and mixtures, listed in Table 4. As expected, the pure components and mixtures give very similar integration areas of the terminal relaxation, confirming that $G_{N\ exp}^0$ is indeed independent of polydispersity.

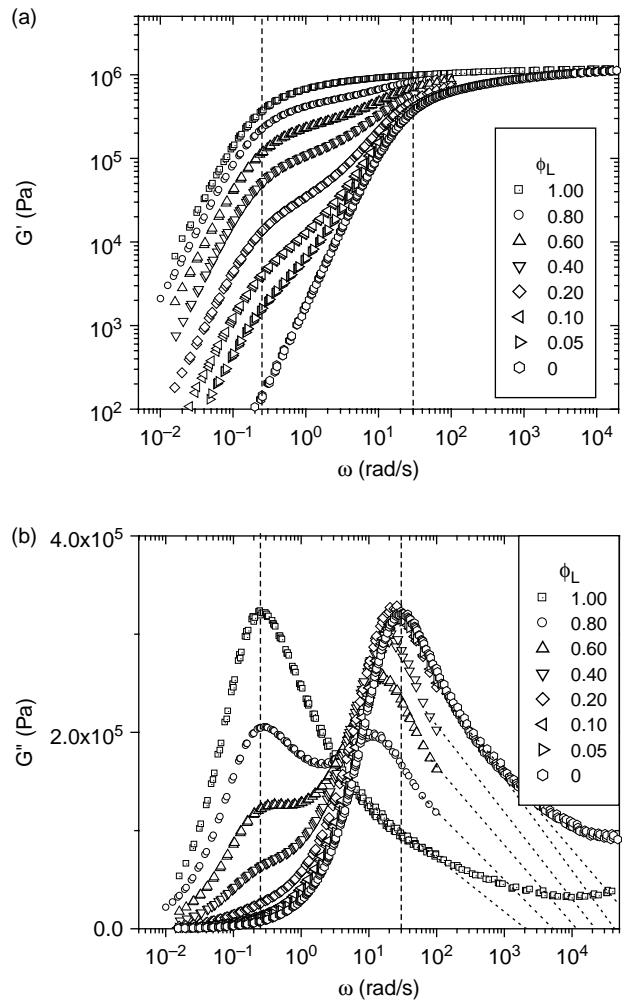Fig. 12. Master curves for (a) G' (log–log plot); and (b) G'' (linear–log plot) of the binary mixtures of PBD 410 K and PBD 100 K at 40 °C. Data obtained from Wang et al. [44]. The dashed lines represent locations of $(\omega_{max})_L$ and $(\omega_{max})_S$ for long and short chains, respectively. Dotted lines represent the extrapolation of G'' at the high frequencies.

5.2. How does polydispersity influence the determination of $G_{N\ exp}^0$?

Although polydispersity does not influence the plateau modulus by itself, it makes it more difficult to correctly extract $G_{N\ exp}^0$ from the data. This is illustrated by the case of commercial polyisobutylene (PIB) with broad MWD. The molecular characterization of the tested Oppanol samples is listed in Table 5. Fetters et al. [87] report a $G_{N\ exp}^0$ value of 0.318 MPa for narrow MWD linear PIB. This value is consistent with 0.29 MPa reported in [17] for linear PIB and [85] for 6-arm star PIB. A corresponding molecular weight between entanglements of about 5700 g/mol can be calculated from Eq. (1) ($\rho = 918$ kg/m³ at 25 °C). Hence, the tested Oppanol B-15, B-50 and B-150 samples have $Z\,(M_n/M_e)$ values of 7.2, 21 and 75, respectively. Plateau modulus values have been obtained for those samples by different methods according to Eqs. (4),(5),(7),(8) and (10). The results are listed in Table 5 and are discussed below.

5.2.1. MIN method extended to polydisperse polymers

Fig. 13(a) shows the master curves at 25 °C of the three tested PIB samples. The visual G' plateau is not frequency-independent especially for the lowest MW sample. Second, the G'' downward slope at $\omega > \omega_{max}$ decreases with decreasing MW and even becomes positive due to the overlap of terminal relaxation processes from different MW components with the high frequency Rouse relaxation. Therefore, the frequency ω_{min} at the minimum of G'' becomes indistinct and results in a big uncertainty for determination of $G^0_{N \, exp}$. This is the same problem as for low MW monodisperse samples, only made worse by polydispersity. From the MIN method (Eq. (4)), we find $G^0_{N \, exp}$ values of 0.280 and 0.312 MPa for B50 and B150, respectively. For sample B15, so there is no terminal maximum for G'' nor a minimum due to the poor level of entanglements ($M_n/M_e = 7.2$).

If we use the modified MIN method by taking $G^0_{N \, exp}$ as G' at the frequency where $\tan \delta$ reaches a minimum ($\omega_{min\_\tan \delta}$) instead of the frequency where G'' reaches a minimum ($\omega_{min\_G''}$), we always obtain a higher value, as shown in Table 5. By using Eq. (7) instead of Eq. (4), we allow the contributions from high-frequency Rouse modes to more or less compensate for the fast terminal relaxation of low MW components. It can, therefore, be understood that Lomellini [57] reports almost constant plateau modulus values calculated by the modified MIN method (0.195–0.209 MPa) for

monodisperse PS with Z ranging from 2 to 50. This approximate compensation mechanism does however not constitute a guaranty of accuracy in all cases.

5.2.2. INT method extension to polydisperse polymers

For the B150 PIB sample, the terminal and Rouse relaxations are well separated and the 'Rouse' slope of G'' above ω_{min} is easily determined (0.67). We use the same exponent to extrapolate the high frequency relaxations for all three samples (shown as thin line in Fig. 13(a)). In this way, the Rouse relaxation can be subtracted from the total relaxation, and the pure terminal relaxation peak can be obtained in Fig. 13(b).

For high MW samples B150 and B50, the $G^0_{N \, exp}$ values obtained by the INT method are very close the literature result obtained for monodisperse PIB (0.31 MPa) [87] and are also in good agreement with the results of the MIN method for the highest MW sample B150. This demonstrates that our Rouse subtraction procedure works well for broad MWD systems. On the other hand, due to the poor level of entanglements, a low $G^0_{N \, exp}$ is again obtained for the lowest MW sample B15.

The modified INT method according to Eq. (8), i.e. integration up to G''_{max} with the assumption of a symmetric peak, as usual underestimates the plateau modulus (Table 5).

Semicrystalline polymers, such as the industrially important polyolefins, have a narrow temperature window for rheological measurements, because they can only be tested above their melting point rather than the glass transition [28,72,88]. Even for high MW samples, it is impossible to observe the plateau region and the high-frequency Rouse region. Therefore, it is also impossible to subtract the Rouse contributions from the terminal peak in the way described above. Hence, when applying the INT method to semicrystalline polymers, the extrapolation of the terminal peak at the high frequency side becomes a difficult problem. This is illustrated by PE and PP examples taken from literature [22,88] and shown in Fig. 14. Significant guesswork is necessary to extrapolate the high-frequency side of the terminal peaks. A wrong extrapolation will result in a large error on the plateau modulus $G^0_{N \, exp}$, as seen Fig. 14(b) for the s-PP case [88,89]. A rough criterion for the extrapolation procedure is that the extension beyond measured data should not exceed 4 decades for samples with MWD below 3. This criterion has been validated for the PIB, PE and s-PP samples presented above as well as simulation results for broad MWD systems to be discussed in next subsection.

Fig. 13. (a) Master curves for three polydisperse PIB samples at 25 °C; (b) linear–log plot for G'', the thin lines represent the pure terminal relaxation after removing the contributions of Rouse modes with an exponent of 0.67.

5.2.3. MAX method extended to polydisperse polymers

Since, MWD influences the shape of the terminal peak, the K constant in the empirical Eq. (6) should depend on polydispersity. A cursory examination of the polydisperse PIB mastercurves shown in Fig. 13 immediately leads to the qualitative conclusion that K increases with polydispersity.

Owing to the recent developments of tube models [13,16,31], it is now possible to predict the influence of MWD on the shape of the terminal peak. We have used the model published by van Ruymbeke et al. to predict the
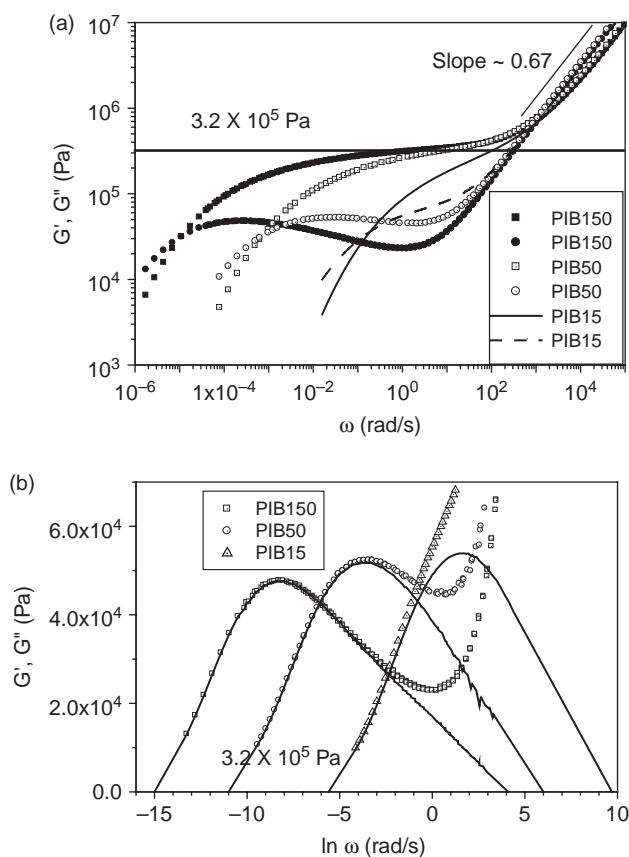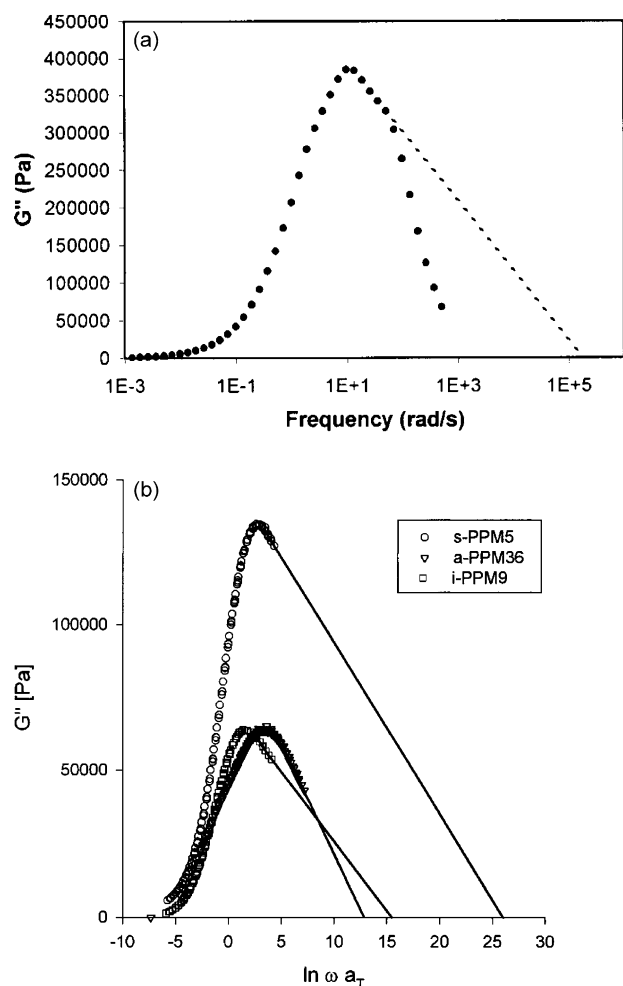
Fig. 14. (a) Extrapolation of G'' for PE (HDL4) [22]; (b) extrapolation of G'' for three kinds of PP [88]. Reprinted from Macromolecules 2000:33;7489 [22] and 1998:31;1335 [88] with permission of the American Chemical Society.

Fig. 15. (a) Normalized terminal relaxation curves G''/G_N^0 vs. ω/ω_{max} predicted by tube model [13,31] for long chains with $Z=200$ and $M_w/M_n=1.01$, 1.1, 1.5, 2, 3 and 5: log–log plot; (b) Ratio of G_N^0/G''_{max} as a function of M_w/M_n: theoretical predictions vs. experiments (data in Table 10).

dynamic moduli at 170 °C for PS samples all with the same number of entanglements ($Z=200$) but with polydispersity indices ranging from 1.01 to 5. The shape of the MWD was assumed to follow the GEX function [11]. Corresponding G'' terminal relaxation peaks are shown in Fig. 15(a). With increasing M_w/M_n, terminal relaxation peaks become broader and G''_{max} decreases. As expected, numerical integration of the whole terminal peak yields the same $G_{N\,exp}^0$ for all samples, confirming that the plateau modulus is independent of polydispersity. As G''_{max} decreases with increasing M_w/M_n, K in Eq. (6) correspondingly increases. Predicted values for K are listed in Table 6, and plotted vs. MWD in Fig. 15(b). As expected, K equals to 3.5–3.8 for nearly monodisperse polymers ($M_w/M_n<1.1$), which agrees well with the experimental observations reported in Section 4.

Since, polydispersity is usually around 2 for condensation polymers or metallocene polyolefins, this case is of particular interest. Recent experimental results [22,26,72,84,89] indicate that the value of K is about 5 for polymers with $M_w/M_n\cong2$. For example, Garcia-Franco et al. [72] recently reported rheological results for metallocene catalyzed ethylene–octene
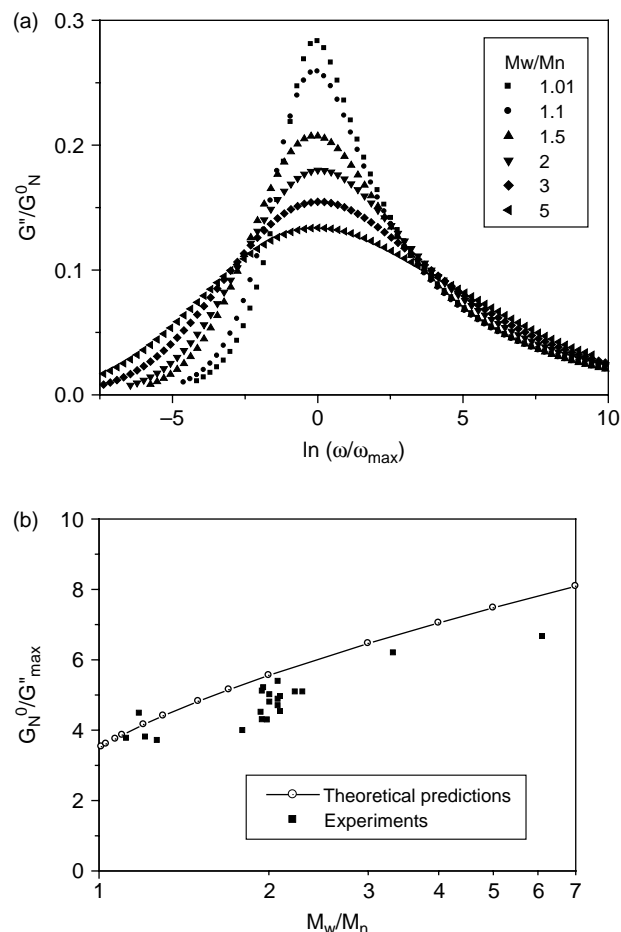
copolymers (EOCs) with a wide range of octene concentration (9.6–75 mol%) but similar polydispersity around 2. The corresponding molecular characteristics and rheological data are reported in Table 7. All samples exhibit a G'' maximum but no minimum, for G'' nor for tan δ, due to the narrow accessible dynamic range. Therefore, the MIN method cannot be used to estimate the plateau modulus. However, both the INT and MAX methods show fairly good agreement. The value of K calculated from the ratio of $G_{N\,exp}^0$ to G''_{max} is 4.8 ± 0.4.

On the other hand, the model published by van Ruymbeke et al. [13,31] predicts a K factor around 5.5 for $M_w/M_n=2$. This small discrepancy between the predicted and observed value possibly arises from a slight mismatch between the experimental and simulated MWDs and/or some deficiency in the mixing law. Interestingly, a comparison with a broad set of data in Table 10 indicates that the model slightly overpredicts the value for K across the board for all polydispersities above 2, as seen in Fig. 15(b). In fact, the M_w/M_n dependence of K as well as the same dependence for the viscosity η_0 [16] are probably the two simplest methods to test mixing laws for polydisperse polymers.

Table 10
Plateau moduli $G_{N\,exp}^0$ (10^5 Pa), G_{max}'', and G_{Nexp}^0/G_{max}'' as a function of M_w/M_n for polydisperse polymers

Sample[a]	$G_{N\,exp}^0$ [b]	G_{max}''	G_{Nexp}^0/G_{max}''	M_w (kg/mol)	M_w/M_n	Ref. and polymers
SNPA-5	15.8	4.2	3.76	265	1.12	[18] PE
HDL4	19.	3.9	4.87	329	2.08	[22] PE
PE800	20.7	5.2	3.98	800	1.80	[26] PE
s-PP32	8.25	1.76	4.69	320	2.08	[89]
s-PP36	8.89	1.75	5.08	363	2.30	s-PP
s-PP44	9.09	1.79	5.08	443	2.23	
1-6a	23.5	5.3	4.47	569	1.18	[93]
2-227a	17.6	4.6	3.80	641	1.21	EPCs
2-12	18.3	4.9	3.70	680	1.27	
EO30	12.7	2.96	4.29	129	1.95	[72]
EO38	8.1	1.89	4.29	173	1.99	EOCs
EO44	7.9	1.58	5.00	197	2.01	
EO52	5.7	1.19	4.79	233	2.01	
EO56	4.6	0.93	4.95	285	2.10	
EO70	2.5	0.49	5.10	941	1.95	
EO87	1.3	0.25	5.20	1270	1.96	
EO92	0.90	0.20	4.50	1080	1.94	
B150	3.18	0.478	6.65	2600	6.12	PIB[c]
B50	3.20	0.517	6.19	400	3.33	
B15	2.90	0.539	5.38	85	2.08	
A2700	2.17	0.48	4.52	35	2.10	Idemitsu PC

[a] Codes in original references.
[b] Estimated by using "INT" method of Eq. (5).
[c] M_v (viscosity-average) and M_v/M_n.

Finally, as discussed above, the fact that the Marvin–Oser formula [59] gives the right value of K for $M_w/M_n = 2$ appears to be a mere coincidence.

5.2.4. Crossover modulus-based methods

When the MWD is very broad MWD and/or the MW very low, especially if the polymer is semicrystalline, G'' will sometimes have no maximum, nor a minimum. This is typically the case for semicrystalline polycondensates and ring opening polymers, e.g. poly (caprolactam) (N6), poly(hexamethylene adipamide) (N66), poly(ethylene terephthalate) (PET), and polyoxymethylene (POM) [28]. In such cases, none of the above methods is applicable. However, alternatives relating the plateau modulus to the terminal crossover point ($G_x = G' = G''$ at the frequency $\omega = \omega_x$) have been proposed by Wu [28] (Eq. (10)) and Nobile–Cocchini [11] (Eq. (11)). The Wu and Nobile–Cocchini relationships have been used to estimate the plateau modulus of the EOC samples [72]. The results are reported in Table 7 and plotted vs. comonomer content in Fig. 16. Wu's method underestimates $G_{N\,exp}^0$ at low comonomer content (<20% octene), while Nobile–Cocchini's method systematically underestimates $G_{N\,exp}^0$ at all comonomer concentrations. $G_{N\,exp}^0$ decreases with increasing comonomer content, which qualitatively agrees the predictions of the packing length model [40,72].

Predictions of van Ruymbeke's model for the $G_{N\,exp}^0/G_x$ ratio are plotted as a function of MWD in Fig. 17 and compared with the Wu and Nobile–Cocchini relationships. Large

differences between the methods can be observed for the $G_{N\,exp}^0/G_x$ ratios. All this suggests that the crossover-based methods are only tentative, mainly due to three factors: the experimental uncertainty on the determination of G_x, the uncertainty on SEC data and the approximations included in the relationships. So plateau modulus values obtained from the crossover methods are best used for qualitative comparisons only.

In summary, polydispersity causes a big uncertainty about the evaluation of $G_{N\,exp}^0$, especially when high-MW samples are unavailable or the accessible dynamic range is limited
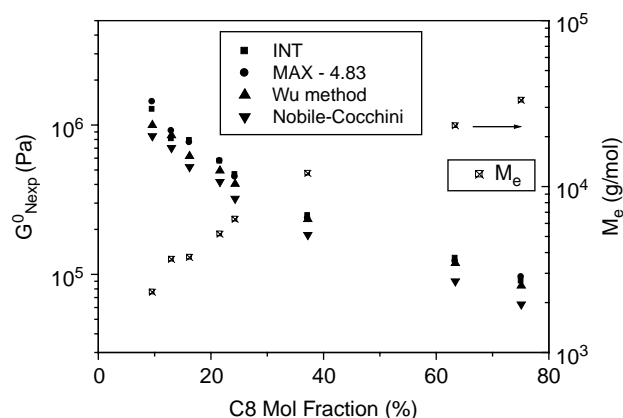
Fig. 16. $G_{N\,exp}^0$ and M_e obtained by different methods as a function of the octene content in EOC copolymers. Data were obtained from Ref. [72].
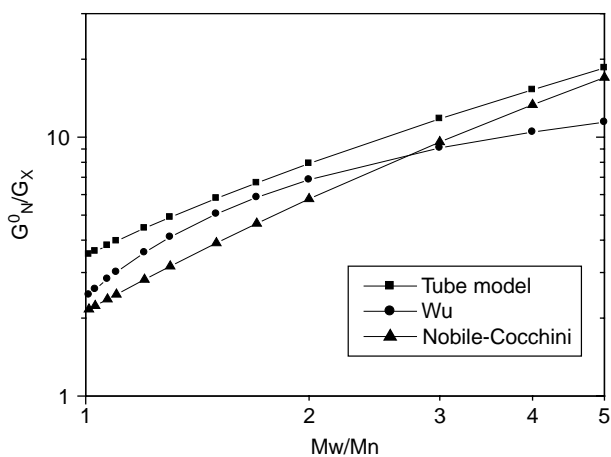
Fig. 17. G_N^0/G_x as a function of M_w/M_n. Comparison between predictions of tube model [13,31] and empirical relationships [11,28].

(semicrystalline polymers). The preferred method is the integration of the G'' terminal peak (INT method) since it does not require any additional approximations, unlike the phenomenological relations between the plateau modulus and G''_{max} or G_x. However, the key problem for the integration method is the correct separation of the terminal relaxation peak from the partially overlapping high-frequency Rouse relaxation. When possible, the subtraction of the Rouse modes or the validity criterion for the extrapolation of G'' at high frequencies should be used. The other methods presented in this section are best used as supplement and/or confirmation. A cross-check between different methods is to be recommended for maximal accuracy.

5.3. Important examples of polydisperse systems

5.3.1. Polyethylene

Although PE has the simplest chain structure among all polymers, there are widely different values reported in literature for its plateau modulus. The problem is twofold. On the one hand, PE can be prepared by various routes (radical, classical transition metal catalysts, metallocene catalysts…) which generate different microstructures and, in most cases, broad MWD. On the other hand, semicrystalline PE has a narrow temperature window for rheological measurements, so only ultra high MW samples will actually show the plateau region. Hydrogenated polybutadiene (HPB) is still considered the best approximation of a model narrow disperse polyethylene, despite the presence of ethyl branches resulting from 1–2 addition during PB synthesis. Fractionation is also used as a route to low polydispersity model samples, but the process for semicrystalline PE with high MW is very difficult and tedious.

Available data from different sources are collected in Table 8. In the literature, the generally accepted value for HDPE is 2.3 MPa [17]. This is the average plateau modulus from various HPB samples with M_w between 187 and 360 kg/mol [19].

Another widely used value is the one proposed by Fetters et al. [21], i.e. 2.6 MPa, which is also estimated from HPB samples as an extrapolation to zero vinyl content (from 1 to 2 addition) at 100 °C [20]. However, the extrapolation is doubtful for two reasons. First, the experimental plateau modulus values show a non linear dependence at low vinyl content. Second the $G_{N\ exp}^0$ values used for extrapolation were measured at $T = 100$ °C, and low vinyl HBP samples show slightly decreasing vertical shift factors (for G''_{max}) with increasing temperature (Table 5 in Ref. [20]). Therefore, the value of 2.6 MPa is possibly overestimated.

Recently, Lohse et al. [23] reported an average $G_{N\ exp}^0$ value of 1.97 MPa for HPB with M_w ranging from 127 to 789 kg/mol, all results obtained by the INT method (Table 8). If the 2.45 MPa outlier for the lowest MW sample (PEL125 in Ref. [23]), possibly due to contamination by Rouse modes, is taken out, all values range from 1.75 to 2.00 MPa and hence are consistent with each other within an uncertainty of 10%. This has to be compared with a big scatter from 1.83 to 2.73 MPa in Ref. [19].

The average value of 1.97 MPa also agrees well with the results for metallocene PEs reported by Wood-Adams et al. and Vega et al. In Ref. [22], the authors use numerical integration of the terminal peak completed by extrapolation at high frequency (in agreement with our validity criterion), as seen in Fig. 14(a). They obtain 1.9 MPa for $G_{N\ exp}^0$. Using the MIN method on the same sample yields an identical value. Finally, the MAX method with a factor $K = 4.8$ valid for polymers with $M_w/M_n \sim 2$ yields 1.88 MPa. So the three methods provide consistent results. In Ref. [26], ultra high MW PE samples with $M_w = 800$ and 3600 kg/mol show a plateau at high frequencies, as a consequence of the extreme large Z. The visual plateau is at 1.92 and 1.95 MPa, respectively. Numerical integration of the terminal peak yields 1.9 MPa for the 800 kg/mol sample. On the other hand, the terminal region could not be reached experimentally for the 3600 kg/mol samples making the INT method impossible for that sample.

Lastly, Vega et al. [24,25] also reports very low $G_{N\ exp}^0$ values around 1.05 MPa for a series of metallocene polyethylenes. Such low values are completely out of the reasonable range and could come either, from a disentangled state in samples supplied as nascent powder [90], from sample inhomogeneities [91], or even from possible transducer compliance problem [74].

In conclusion, the reasonable $G_{N\ exp}^0$ value for PE is close to 2.0 MPa. A strong evidence for this value is that ultrahigh molecular weight PE with $Z \sim 3000$ (3600 kg/mol sample PE3600K in Ref. [26]) exhibits a visual plateau at $G' \sim 1.95$ MPa nearly independent of frequency. The corresponding entanglement molecular weight of PE, calculated from Eq. (1), is thus 1200 g/mol at 190 °C ($\rho = 0.760$ g/cm^3).

5.3.2. Bisphenol-A polycarbonate

PC is a classical example of a condensation polymer, hence high MW and narrow MWD samples are very difficult to prepare. Available data for PC from different sources are collected in Table 9. The scatter of published $G_{N\ exp}^0$ values is very large indeed as it ranges from 1.2 to 4.1 MPa [21,27–31].
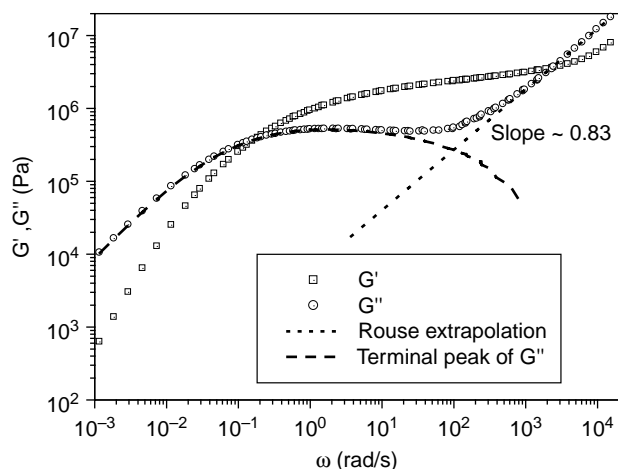
Fig. 18. Master curve for PC-A2700 at 180 °C. The dashed line represents the pure terminal relaxation after removing the contributions of Rouse modes with an exponent of 0.83.

The first experimental estimate (from 1.71 to 1.96 MPa) was obtained from tensile stress relaxation experiments [27]. Wu [28] and Wimberger-Friedl et al. [29] independently reported $G_{N\ exp}^0$ estimates around 2.0–2.2 MPa by the tan δ minimum method for average M_w PC samples (33 and 48 kg/mol). In contrast, an exceptionally high value of 4.07 MPa was extracted by a BSW spectrum fitting method [30] on high *MW* PC (150 kg/mol). On the other hand, a low value of 1.2 MPa was obtained by a tube model fitting procedure for a fractionated sample with a M_w of 39 kg/mol [31].

The commonly used value today is 2.7 MPa reported by Fetters et al. [21], based on the packing length model. This value agrees with recent multiscale simulations [92].

We have investigated the LVE behavior of PC over a temperature range from 160 to 210 °C at about 20 °C intervals. The sample tested (PC-A2700 in Table 9) has a M_w of 35 kg/mol and M_w/M_n–2.1. The master curve is presented in Fig. 18. We use all three methods for the determination of $G_{N\ exp}^0$. For the INT method, we subtract the Rouse contributions, shown as a thin line in Fig. 18, to obtain the pure G'' terminal peak. The experimental 'Rouse' slope is very high (0.83). For the MAX method, we use a value of 4.8 for the constant *K*. $G_{N\ exp}^0$ values of 2.29, 2.17, and 2.32 are obtained by the MIN, INT and MAX methods, respectively, indicating excellent consistency. The average is about 2.25 MPa, significantly lower than 2.7 MPa commonly used, but in fact consistent with the majority of literature results [28,29].

6. Conclusions

The plateau modulus is perhaps the most fundamental parameter describing the linear viscoelasticity of entangled macromolecules, in particular from the vantage point of tube models, since it is directly linked to the molecular weight between entanglements. In this paper, we have tested and compared all major published methods for the experimental determination of G_N^0 for monodisperse as well as polydisperse polymers with a linear architecture.

For long-chain linear monodisperse model systems ($M_w/M_n < 1.1$ and $Z > 20$–30), such as anionically polymerized PBD, PI and PS, the situation is quite satisfactory since there is excellent agreement between the various methods, within an error margin of 5–10% close to the experimental uncertainty. For low *MW* samples, the 'integration' method requires a careful extrapolation at the high frequency side. This is best achieved by a simple subtraction of the high frequency Rouse relaxation. The universal terminal relaxation concept is validated for long chains, in logical agreement with tube model concepts. On the other hand, the observed *MW* dependence of $G_{N\ exp}^0$ is very weak compared with recent predictions [3,46,77], which indicates an overestimation of CLF effects in recent tube models.

Polydispersity introduces a large uncertainty about the estimation of $G_{N\ exp}^0$, which is quite significant from the practical point of view, since numerous polymers cannot be synthesized with $M_w/M_n < 2$. We have analyzed the extension to polydisperse polymers of the methods validated for monodisperse systems. This has been illustrated by several important examples, such as PIB, PC and PE. Agreement within an error margin of 15% could be achieved as a result of careful measurements and the correct use of the methods. The preferred scheme is the terminal peak integration, but a prerequisite is the correct separation of the terminal behavior from the partially overlapping high frequency Rouse relaxation modes. The Rouse modes subtraction procedure validated for monodisperse samples can be used if the experimental data extend high enough into the Rouse regime. In most cases, the terminal peak has to be extrapolated at high frequencies. The extrapolation should not exceed four decades on the frequency scale. Methods based on the 'crossover' modulus are only semiquantitative. Predictions of $G_{N\ exp}^0$ for highly polydisperse systems from tube models have to be evaluated critically since they still suffer from uncertainties about mixing laws and accuracy of the MWD description. A cross-check of all available methods is the best way to achieve maximal accuracy for polydisperse systems.

References

[1] (a) de Gennes PG. J Chem Phys 1971;55:572.
     (b) de Gennes PG. Scaling concepts in polymer physics. Ithaca: Cornell University Press; 1979.

[2] Doi M, Edwards SF. The theory of polymer dynamics. Oxford: Clarendon Press; 1986.

[3] Likhtman AE, McLeish TCB. Macromolecules 2002;35:6332.

[4] Larson RG, Sridhar T, Leal LG, McKinley GH, Likhtman AE, McLeish TCB. J Rheol 2003;47:809.

[5] Watanabe H. Prog Polym Sci 1999;24:1253.

[6] McLeish TCB. Adv Phys 2002;51:1379.

[7] Rubinstein M, Colby RH. Polymer physics. New York: Oxford University Press; 2003.

[8] Wu S. Macromolecules 1985;18:2023.

[9] Wasserman SH, Graessley WW. Polym Eng Sci 1996;36:852.

[10] Maier D, Eckstein A, Friedrich C, Honerkamp J. J Rheol 1998;42:1153.

[11] Nobile MR, Cocchini F. Rheol Acta 2001;40:111.

[12] Leonardi F, Allal A, Marin G. J Rheol 2002;46:209.

[13] van Ruymbeke E, Keunings R, Bailly C. J Non-Newtonian Fluid Mech 2002;105:153.

[14] Park SJ, Larson RG. J Rheol 2003;47:199.

[15] Guzman JD, Schieber JD, Pollard R. Rheol Acta 2005;44:342.

[16] Laun HM, Leonardi F, Carrot C, van Ruymbeke E, Keunings R, Bailly C, et al. In: Proceeding of 2nd Annual European Rheology Conference, Grenoble, France, April 21–23; 2005. p. 155.

[17] Ferry JD. Viscoelastic properties of polymers. 3rd ed. New York: Wiley; 1980.

[18] Raju VR, Smith GG, Marin G, Knox JR, Graessley WW. J Polym Sci, Polym Phys Ed 1979;17:1183.

[19] Raju VR, Rachapudy H, Graessley WW. J Polym Sci, Polym Phys Ed 1979;17:1223.

[20] Carella JM, Graessley WW, Fetters LJ. Macromolecules 1984;17:2775.

[21] Fetters LJ, Lohse DJ, Richter D, Witten TA, Zirkel A. Macromolecules 1994;27:4639.

[22] Wood-Adams PM, Dealy JM, deGroot AW, Redwine OD. Macromolecules 2000;33:7489.

[23] Lohse DJ, Milner ST, Fetters LJ, Xenidou M, Hadjichristidis N, Mendelson RA, et al. Macromolecules 2002;35:3066.

[24] Aguilar M, Vega JF, Sanz E, Martinez-Salazar J. Polymer 2001;42:9713.

[25] Vega JF, Aguilar M, Martinez-Salazar J. J Rheol 2003;47:1505.

[26] Vega JF, Rastogi S, Peters GWM, Meijer HEH. J Rheol 2004;48:663.

[27] Mercier JP, Aklonis JJ, Litt M, Tobolsky AV. J Appl Polym Sci 1965;9:447.

[28] Wu S. J Polym Sci, Polym Phys Ed 1989;27:723.

[29] Wimberger-Friedl R, Hut MGT, Schoo HFM. Macromolecules 1996;29:5453.

[30] Jackson JK, Winter HH. Rheol Acta 1996;35:645.

[31] van Ruymbeke E, Keunings R, Stephenne V, Hagenaars A, Bailly C. Macromolecules 2002;35:2689.

[32] Kavassalis TA, Noolandi J. Phys Rev Lett 1987;59:2674.

[33] Kavassalis TA, Noolandi J. Macromolecules 1988;21:2869.

[34] Kavassalis TA, Noolandi J. Macromolecules 1989;22:2709.

[35] Masubuchi Y, Ianniruberto G, Greco F, Marrucci G. J Chem Phys 2003;119:6925.

[36] Graessley WW, Edwards SF. Polymer 1981;22:1329.

[37] Milner ST. Macromolecules 2005;38:4929.

[38] Fetters LJ, Lohse DJ, Graessley WW. J Polym Sci, Polym Phys Ed 1999;37:1023.

[39] Fetters LJ, Lohse DJ, Milner ST, Graessley WW. Macromolecules 1999;32:6847.

[40] Fetters LJ, Lohse DJ, Garcia-Franco CA, Brant P, Richter D. Macromolecules 2002;35:10096.

[41] Wischnewski A, Monkenbusch M, Willner L, Richter D, Likhtman AE, McLeish TCB, et al. Phys Rev Lett 2002;88:058301.

[42] Padding JT, Briels WJ. J Chem Phys 2004;120:2996.

[43] Likhtman AE. Macromolecules 2005;38:6128.

[44] Wang S, Wang SQ, Halasa A, Hsu WL. Macromolecules 2003;36:5355.

[45] Lee JH, Fetters LJ, Archer LA. Macromolecules 2005;38:4484.

[46] Milner ST, McLeish TCB. Phys Rev Lett 1998;81:725.

[47] McLeish TCB, Milner ST. Adv Polym Sci 1999;143:195.

[48] Marrucci G, Greco F, Ianniruberto G. Curr Opin Colloid Interface Sci 1999;4:283.

[49] Berek D, Bruessau R, Lilge D, Mingozzi I, Podzimek S, Robert E., IUPAC Round Robin Tests of SEC. [http://wwwiupacorg/projects/posters01/berek01pdf].

[50] Gahleitner M. J Macromol Sci, Pure Appl Chem 1999;A36:1731.

[51] Sanders JF, Ferry JD. Macromolecules 1969;2:440.

[52] Raju VR, Menezes EV, Marin G, Graessley WW, Fetters LJ. Macromolecules 1981;14:1668.

[53] Struglinski MJ, Graessley WW. Macromolecules 1985;18:2630.

[54] Tao H, Huang C, Lodge TP. Macromolecules 1999;32:1212.

[55] Wu S. J Polym Sci, Polym Phys Ed 1987;25(557):2511.

[56] Wu S, Beckerbauer R. Polymer 1992;33:509.

[57] Lomellini P. Polymer 1992;33:1255.

[58] Onogi S, Masuda T, Kitagawa K. Macromolecules 1970;3:109.

[59] (a) Marvin RS, Oser H. J Res Nat Bur Stand 1962;66B:171.
    (b) Oser H, Marvin RS. J Res Nat Bur Stand 1963;67B:87.

[60] Colby RH, Fetters LJ, Graessley WW. Macromolecules 1987;20:2226.

[61] Colby RH, Fetters LJ, Funk WG, Graessley WW. Macromolecules 1991;24:3873.

[62] Baumgaertel M, De Rosa ME, Machado J, Masse M, Winter HH. Rheol Acta 1992;31:75.

[63] Gotro JT, Graessley WW. Macromolecules 1984;17:2767.

[64] Santangelo PG, Roland CM. Macromolecules 1998;31:3715.

[65] Matsumiya Y, Watanabe H, Osaki K. Macromolecules 2000;33:499.

[66] Watanabe H, Matsumiya Y, Kanaya T, Takahashi Y. Macromolecules 2001;34:6742.

[67] Watanabe H, Ishida S, Matsumiya Y, Inoue T. Macromolecules 2004;37:1937.

[68] Watanabe H, Ishida S, Matsumiya Y, Inoue T. Macromolecules 2004;37:6619.

[69] Abdel-Goad M, Pyckhout-Hintzen W, Kahle S, Allgaier J, Richter D, Fetters LJ. Macromolecules 2004;37:8135.

[70] Graessley WW, Roovers J. Macromolecules 1979;12:959.

[71] Schausberger A, Schindlauer G, Janeschitz-Kriegl H. Rheol Acta 1985;24:220.

[72] Garcia-Franco CA, Harrington BA, Lohse DJ. Rheol Acta 2005;44:591.

[73] Liu CY, Li CX, Chen P, He JS, Fan QR. Polymer 2004;45:2803.

[74] Macosko CW. Rheology: principles measurement and applications. New York: Wiley–VCH; 1994.

[75] ARES user manual. New Castle: TA Instruments; 2003.

[76] Baumgaertel M, Schausberger A, Winter HH. Rheol Acta 1990;29:400.

[77] (a) Doi M. J Polym Sci, Polym Lett Ed 1981;19:265.
    (b) Doi M. J Polym Sci, Polym Phys Ed 1983;21:667.

[78] Liu CY, He JS, Keunings R, Bailly C. Macromolecules 2006;39:3093.

[79] Jackson JK, Derosa ME, Winter HH. Macromolecules 1994;27:2426.

[80] Rouse PE. J Chem Phys 1953;21:1272.

[81] (a) des Cloizeaux J. Macromolecules 1990;23:4678.
    (b) des Cloizeaux J. J Phys Lett 1984;45:L17.

[82] des Cloizeaux J. Macromolecules 1990;23:3992.

[83] Greco F. Macromolecules 2004;37:10079.

[84] Aguilar M, Vega JF, Pena B, Martinez-Salazar J. Polymer 2003;44:1401.

[85] Santangelo PG, Roland CM, Puskas JE. Macromolecules 1999;32:1972.

[86] Rubinstein M, Colby RH. J Chem Phys 1988;89:5291.

[87] Fetters LJ, Graessley WW, Kiss AD. Macromolecules 1991;24:3136.

[88] Eckstein A, Suhm J, Friedrich C, Maier RD, Sassmannshausen J, Bochmann M, et al. Macromolecules 1998;31:1335.

[89] Liu CY, Yu J, He JS, Liu W, Sun CY, Jing ZH. Macromolecules 2004;37:9279.

[90] Rastogi S, Lippits DR, Peters GWM, Graf R, Yao YF, Spiess HW. Nat Mater 2005;4:635.

[91] Gahleitner M. Prog Polym Sci 2001;26:895.

[92] Everaers R, Sukumaran SK, Grest GS, Svaneborg C, Sivasubramanian A, Kremer K. Science 2004;303:823.

[93] Fetters LJ, Lee JH, Mathers RT, Hustad PD, Coates GW, Archer LA, et al. Macromolecules 2005;38:10061.

Chen-Yang Liu was born in the Sichuan Province, China, in 1973. He received his bachelor's degree in Polymer Materials and Engineering from the University of Science and Technology of Qingdao in 1994, and his PhD degree in Polymer Science from the Institute of Chemistry, Chinese Academy of Sciences, in 2002 under the guidance of Prof. Jiasong He. The subject of his thesis was the relationship between structure and properties of metallocene olefin copolymers. He next joined the Institute as an assistant professor. He is currently a post-doctoral research associate at Université catholique de Louvain collaborating with Prof Christian Bailly and Prof Roland Keunings. His research interests include dynamics of polymer liquids, rheometry, and rheology of polymer composites.

Jiasong He graduated from University of Science and Technology of China in 1966, and received his M.S. degree in 1981 in Polymer Science from Graduate School, Chinese Academy of Sciences (GSCAS) and Ph.D. degree in 1985 in Polymer Science from Institute of Chemistry, CAS (ICCAS) under the supervision of Professor Renyuan Qian. Since 1981 he has been continuing his work in ICCAS, and became an Associate Professor in 1986 and Professor in 1994. In 1987 he worked as a postdoctoral researcher in DSM Research BV, the Netherlands. Dr He served as Director of State Key Laboratory of Engineering Plastics, ICCAS in 1996, and Professor of GSCAS in 2002. He was a chairman of two international symposia and is resuming for the third one. He has published more than 100 peer-reviewed research papers on polymer blends and composites in fundamental aspects involved such as rheology and processing, orientation and crystallization, morphology evolution and compatibilization, and holds over 10 invention patents. Dr He is sitting at Executive Publishing Committee of two scientific journals (in Chinese and English, respectively), and Council Member, Polymer Division, Chinese Chemical Society; Council Member, Chinese Society of Composite Materials; Member of International Union of Pure and Applied Chemistry (IUPAC) Subcommittee on Macromolecular Terminology and Subcommittee on Structure and Properties of Commercial Polymers. In 1997 he received Wang Baoren Award for Accomplishment in Basic Research in Polymer Science, Chinese Chemical Society.

Evelyne van Ruymbeke obtained a Masters degree in Applied Mathematics at Université catholique de Louvain, Belgium in 2000. In 2005, under the supervision of Profs. Christian Bailly and Roland Keunings, she received a PhD from the same university. The subject of her thesis was the relationship between linear viscoelasticity and structure of linear and star polymer melts. In 2005, she benefited from a Post-doctoral European Marie Curie fellowship. She is currently a post-doctoral researcher at FORTH, Institute of Electronic Structure & Laser, Heraklion, Crete, Greece, with Prof. Dimitris Vlassopoulos. Her main research interests include understanding the relationship between rheology and structure of complex architecture polymer melts and exploring the relationship between structure and dynamics of soft colloidal systems.

Roland Keunings following a Masters degree in Applied Mathematics in 1979, obtained a PhD in 1982 at the Université catholique de Louvain, Belgium under the supervision of Prof. M. Crochet. From 1983 to 1988, he successively served as Research Fellow and Divisional Fellow at the University of California, Berkeley, USA. He next became Lecturer at the Université catholique de Louvain and was promoted Full Professor in 1996. He is currently Prorector for Research of the same university. Prof. Keunings is the author or co-author of 136 scientific publications and has given 23 plenary and keynote lectures at international symposia. He is Co-Editor in Chief of the Journal of Non-Newtonian Fluid Mechanics. He has received the Weissenberg Award of the European Society of Rheology in 2005. Prof. Keunings' recent research interests cover various aspects of computational rheology, non-Newtonian fluid mechanics, mesoscale modelling of polymer melts and solutions, micro-macro simulations, non-linear finite elements methods and parallel numerical algorithms.

Christian Bailly received a Masters degree in Applied Physics in 1979, followed by a PhD in Polymer Science in 1983 at Université catholique de Louvain, Belgium. After serving in 1984–85 as a postdoctoral Research Associate at the University of Massachusetts, Amherst, USA, in the team of Profs. W. McKnight and F. Karasz, he joined General Electric Plastics, Bergen op Zoom, the Netherlands, and GE Corporate R&D, Schenectady, NY, USA. Two of his major research areas at that time were the reactive compatibilization of polymer blends and the melt synthesis of polycarbonate. He next joined Université catholique de Louvain as tenured Professor in 1998 and was promoted Full Professor in 2004. Prof. Bailly is the author or co-author of 100 refereed papers, patents or book chapters. His current research interests focus on the influence of macromolecular/supramolecular architecture on the rheology of entangled polymer melts or solutions and the structure-property relationships of multiphasic polymer systems, including nanocomposites.